Climate Dynamics (1997) 13: 247–257

Climate Dynamics

Modeling bio-geophysical feedback in the African and Indian monsoon region

M. Claussen

Potsdam-Institut für Klimafolgenforschung, P. O. Box 601203, D-14412 Potsdam, Germany

Received: 18 April 1995/Accepted: 17 September 1996

Abstract. An asynchronously coupled global atmosphere-biome model is used to assess the dynamics of deserts and drought in the Sahel, Saudi-Arabia and the Indian subcontinent. Under present-day conditions of solar irradiation and sea-surface temperatures, the model finds two solutions: the first solution yields the present-day distribution of vegetation and deserts and the second shows a northward spread of savanna and xerophytic shrub of some 600 km, particularly in the southwest Sahara. Comparison of atmospheric states associated with these solutions corroborates Charney's theory of a self-induction of deserts through albedo enhancement in the Sahel. Over the Indian subcontinent, changes in vegetation are mainly caused by a positive feedback between increased soil moisture and stronger summer monsoon.

1. Introduction

At the second conference on Global Climate Change and Variability, Shukla (1992) gave a review of GCM (general circulation model) response to changes in the boundary conditions at the earth's surface. In particular, Shukla mentioned that 'Charney's cycle' has not yet been closed by modelers, referring to Charney's (1975) theory of a positive bio-geophysical feedback of desertification.

Charney (1975) and, subsequently, Charney et al. (1975, 1977) suggested that a desert feeds upon itself in the following manner: sandy, non-vegetated soil has much higher albedo than soil covered by vegetation. Therefore a desert reflects more solar radiation to space than its vegetated surrounding under the same meteorological conditions. Moreover, desert surfaces are hotter than vegetated surfaces, and the air above is less cloudy. Hence a desert emits more longwave radiation to space. The net result is that a desert is a radiative sink of heat relative to its surroundings. In order to maintain thermal equilibrium, the air must descend and compress adiabatically. Consequently, the relative humidity of the air decreases and the likelihood of precipitation becomes vanishingly small.

Numerical models (e.g. Charney et al. 1975, 1977) support the general hypothesis that increasing surface albedo could reduce precipitation. On the other hand, they did not support the detailed mechanism Charney suggested, except for the Sahel (Dickinson 1992). Dickinson points out that in most semi-arid regions, it depends on the details of the regional climate whether changes in moisture convergence would enhance or cancel the effects of increased evapotranspiration in modifying precipitation. Moreover, Dickinson (1992) criticizes that Charney's original hypothesis includes only the role of atmospheric moisture convergence, but not surface moisture fluxes.

Previous discussion on desert dynamics is based on sensitivity studies in which the response of the atmosphere to prescribed land-surface conditions is analyzed. What has been missing is the modeling of the response of vegetation to a change in precipitation and, in turn, the response of the atmosphere to a change in vegetation. Meanwhile, first attempts have been undertaken to incorporate continental vegetation as an interactive component of a global climate model (Henderson-Sellers 1993; Claussen 1994). While Henderson-Sellers (1993) addresses the problem of deforestation, Claussen (1994) focuses on numerical aspects of coupling GCMs with biome models and on the stability of the model system, atmospheric dynamics are not analyzed.

Therefore, the problem of desert dynamics is reassessed by using a coupled atmosphere-biome model. This is done in the following way: firstly by investigating whether the atmosphere-biome model is able to reproduce present-day pattern of global vegetation and deserts. Secondly, the atmosphere-biome model is initialized using a drastic change in tropical and subtropical vegetation, in the following known as 'anomalous initial state'. It is presumed that the model will find a new, 'anomalous solution'. Since the biome model used here is an equilibrium model, it does not take into account succession or migration of vegetation. Hence the equilibrium response of the atmosphere–biosphere system to changes in land-surface conditions will be analyzed by comparing different (equilibrium) solutions of the atmosphere-biome model in terms of biome distributions, atmospheric states as well as

surface energy budgets. In particular, Charney's hypothesis of a positive bio-geophysical feedback in semi-arid regions will be reassessed.

It is anticipated that a large-scale change in tropical and subtropical vegetation will induce a response of the Hadley–Walker circulation. Hence the present investigation addresses a global problem. It is not a study of local succession where small-scale, dynamic vegetation models, gap models for example (e.g., Prentice et al. 1993), are the appropriate tools.

2 The atmospheric model and the biome model

2.1 The atmospheric model

As an atmospheric component of the combined atmosphere-biome model, the climate model ECHAM was taken which was developed at the Max-Planck-Institut für Meteorologie in Hamburg. The model physics as well as its validation is described in detail by Roeckner et al. (1992). In this study, ECHAM is run at T21 resolution, hence the grid at which the vertical transports between the atmosphere and the surface are computed has a resolution of $5.6^\circ \times 5.6^\circ$, i.e. appr. $600\,\text{km} \times 600\,\text{km}$ at the equator. The climate model ECHAM (level 3) is able to simulate most aspects of the observed time-mean circulation and its intraseasonal varability with remarkable skill (Roeckner et al. 1992). Nevertheless, there are a few problems. For example, during the respective summer season, there is too much precipitation over South Africa and Australia and off the west coast of Central America, while the rainfall over India is underestimated during the summer monsoon season. There is a lack of precipitation over the continents in the Northern Hemisphere in the summer, for example over the United States, over Europe, and over the dry regions of Asia. In these areas, the boundary-layer temperatures are generally too high with the largest error of about 6 K.

In the original version of ECHAM (level 3), there are no specific biomes or vegetation types prescribed. Instead, surface parameters which control the energy, momentum and moisture are specified from topographic or satellite data or are taken as global constants. To allow for coupling with a vegetation model, ECHAM was modified in such a way that arbitrary global data of surface parameters, background albedo, roughness length, vegetation ratio, leaf area index, and forest ratio, can be specified.

2.2 The BIOME model

Biomes are computed by using the BIOME model of Prentice et al. (1992). Prentice et al.'s (1992) model is chosen, because this model is based on physiological considerations rather than on correlations between climate distribution and biomes as they exist today. Biomes are not taken as given as in the Holdridge classification for example, but emerge through the albeit parametrized interaction of constituent plants. Therefore, the BIOME model can be applied to the assessment of changes in natural vegetation patterns in response to different climate states.

In the BIOME model, 14 plant functional types are assigned climate tolerances in terms of amplitude and seasonality of climate variables. For example, the cold tolerance is expressed in terms of the coldest monthly mean temperature and the heat requirement, in terms of yearly temperature sums. The BIOME model predicts which plant functional type can occur in a given environment, i.e., in a given set of climate variables. Competition between different plant types is treated indirectly by the application of a dominance hierarchy which effectively excludes certain types of plants from a site, based on the presence of others, rather than being excluded by climate (Cramer 1995). Finally, biomes are defined as combinations of dominant types.

Validation of global biome models is a problem. Using the IIASA climate data base (Leemans and Cramer 1990), Prentice et al. (1992) predict global pattern of biomes which are in fair agreement with the global distribution of actual ecosystem complexes being evaluated by Olson et al. (1983). Where intensive agriculture has obliterated the natural vegetation, comparison of predicted biomes and observed ecosystems is, of course, omitted.

2.3 Coupling the atmospheric model with the BIOME model

ECHAM is asynchronously coupled with the BIOME model: monthly means of near-surface temperature, precipitation, and cloudiness are computed from ECHAM climatology. From these data, a global distribution of biomes is diagnosed by use of the BIOME model. Surface parameters which are defined to control energy and momentum fluxes at the atmosphere – earth interface are allocated to biomes. With the resulting global set of surface parameters an integration with ECHAM is performed. A new climatology from this integration and, subsequently, a new global distribution of biomes is evaluated, and so on. In the following, the sequence of allocation of surface parameters to biomes, integration of the atmospheric model, and computation of biomes is referred to as 'iteration'. Several iterations are performed until the biome patterns and atmospheric states of successive iterations do not reveal any significant trend.

Based on earlier experience (Claussen 1994), the climate simulation in each iteration is carried out over several years. In Claussen (1994) it is shown that there is no significant difference between biome patterns if the climate model is integrated for five or for ten years and if the results of the climate model are fed into the vegetation model at the end of each five or ten year integration. Here, a period of six years is chosen. The first year of each period is taken as spin-up time to allow for soil-water transports to adjust. Hence biomes are computed from the climatology of the remaining five years.

Allocation of surface parameters to biomes is mainly based on earlier literature. A background albedo α (albedo of the snow-free surface), a leaf area index LAI, a forest ratio c_F (fractional cover of a grid cell by forest), and a roughness length of vegetation z_{0v} are specified for each

biome (see Table 1). A vegetation ratio c_v (fractional cover of a grid cell by vegetation) is computed from the empirical relation (see Monteith 1973)

$$c_v = 1 - \exp(-0.4 \times LAI).$$

The surface type *sand desert* does not appear in the original BIOME model of Prentice et al. (1992). It was added to take into account the strong variability in desert albedo, as seen in satellite data (e.g., Ramanathan et al. 1989). In the Sahara and the Arabian penninsula, large patches of high albedo (α larger than 0.3) are found. Therefore, whenever the BIOME model predicts *hot desert* in these areas, then *hot desert* is replaced by *sand desert*. This simple procedure was chosen, because it was not possible to uniquely relate the abundance of *sand desert* to climate and soil texture.

3 The experiment

3.1 Biomes

To assess the problem of multiple solutions of the atmosphere–biosphere system in the tropical region, two experiments are set up; a control run and an anomaly run. The control run and the anomaly run differ only in their initial land-surface conditions.

In the control run, the ECHAM-BIOME model is initialized with the biome distribution which results from a 30-y climatology of the ECHAM model (see Fig. 1). This distribution resembles the biome pattern computed from observed climatology (e.g., Prentice et al. 1992). Differences between the biome distribution estimated from simulation and observation are found in Northern Australia, South Africa, and North America which are related to model deficiencies mentioned in Sect. 2.1 (Claussen and Esch 1994). The atmospheric model, ECHAM, is driven by present-day orbital conditions and by the climatology of the annual cycle of SST (sea-surface temperatures) on average over 1979 to 1988 obtained from the Atmospheric Model Intercomparison Project (AMIP) data set (Gates 1992).

Four iterations are performed for the control run. In Fig. 2, the biome pattern of the last, fourth iteration of the control simulation is shown. The differences between biome distributions of successive iterations as well as between the initial distribution and each iteration period are such that 12% to 16.5% of the total continental surface area without Antarctica differ. These values are as large as the variability found if biomes are computed from different 5-y climate simulations or better, equally likely numerical realizations, of the same climate state (Claussen 1994, 1996). There is no trend in global and individual Kappa statistics when considering differences in biome patterns between successive interactions. (The Kappa statistics are presented by Monserud and Leemans 1992 as an objective tool for comparing global vegetation maps.) Moreover, there is no trend in land area covered by each biome (listed in Table 2). Apparently, the present-day global biome distribution seems to be a stable solution of the ECHAM-BIOME model.

In the anomaly simulation, a new equilibrium-response of the ECHAM-BIOME model is sought by turning the tropical vegetation "upside down": *hot desert* and *sand desert* are replaced by *tropical rain forest* and *tropical rain forest*, *tropical seasonal forest*, and *savanna* by *hot desert*.

With the new, anomalous initial condition, the ECHAM-BIOME "jumps" to a new equilibrium. Except for the first iteration, biome distributions of all successive iterations resemble each other. Five iterations are carried out in the anomaly run. No trend in global and individual Kappa values or land area covered by each biome is found for the last four iterations. The only exception is the *polar desert* which slightly, but significantly, expands its total area. However, the agreement in the geographical distribution of the *polar desert* between successive iterations, as indicated by the individual Kappa statistics, does not reveal any significant trend. The biome distribution resulting from the fifth and last iteration of the anomaly run is plotted in Fig. 3.

Table 2 depicts the land area (in $10^6 km^2$) covered by each biome (note that Antarctica is not included in *polar*

Table 1. Allocation of surface parameters used in the atmospheric model to biomes specified in Prentice et al. (1992) BIOME model

	Biome name	α_v	LAI	c_v	c_F	z_{0v} (m)
01	Tropical rain forest	0.12	9.3	0.98	0.98	2.000
02	Tropical seasonal forest	0.12	4.3	0.82	0.82	2.000
03	Savanna	0.15	2.6	0.65	0.58	0.361
04	Warm mixed forest	0.15	6.0	0.91	0.79	0.716
05	Temperate deciduous forest	0.16	2.7	0.65	0.65	1.000
06	Cool mixed forest	0.15	2.0	0.54	0.54	1.000
07	Cool conifer forest	0.13	9.1	0.97	0.97	1.000
08	Taiga	0.14	3.7	0.77	0.77	0.634
09	Cold mixed forest	0.15	2.0	0.54	0.54	1.000
10	Cold deciduous forest	0.14	3.7	0.77	0.77	0.634
11	Xerophytic woods/shrub	0.18	2.6	0.66	0.19	0.111
12	warm grass/shrub	0.20	0.8	0.27	0.00	0.100
13	cool grass/shrub	0.19	1.0	0.33	0.00	0.055
14	tundra	0.17	1.2	0.37	0.06	0.033
15	hot desert	0.20	0.2	0.09	0.00	0.004
16	cool desert	0.20	0.3	0.10	0.00	0.005
17	ice/polar desert	0.15	0.0	0.00	0.00	0.001
18	sand desert	0.35	0.0	0.00	0.00	0.004

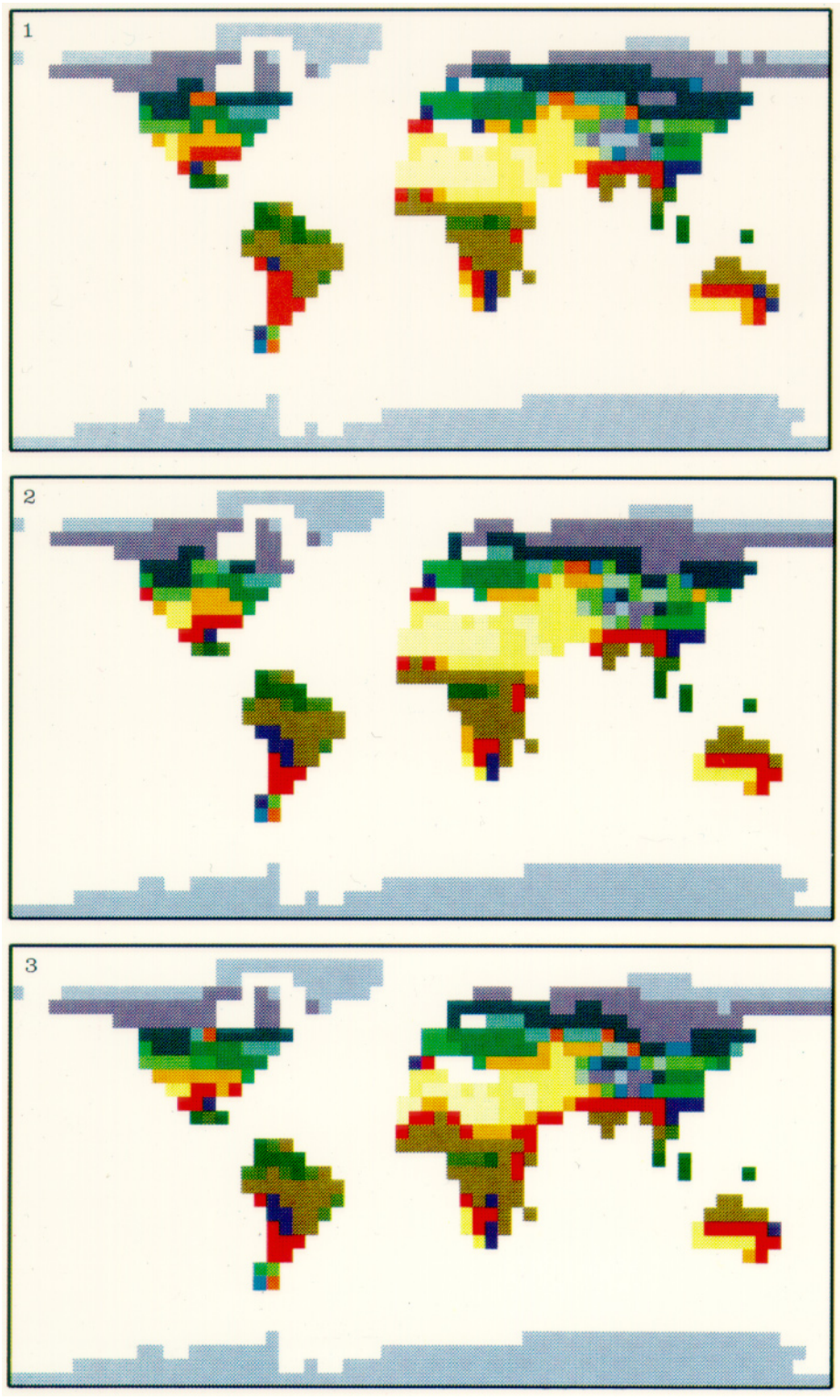

Figs. 1–3. 1. Biome distribution computed from a 30 year simulation of the present-day climate with the Hamburg climate model ECHAM 3. **2.** Biome distribution computed from the fourth (and last) iteration of the atmosphere-biome model when initialized with the present-day biome distribution shown in Fig. 1. **3.** Biome distribution computed from the fifth (and last) iteration of the atmosphere-biome model when initialized with the anomalous biome distribution (see Section 3.1)

desert). In the first four columns, results of the iterations of the control simulation are listed. Columns 5 to 9 refer to the anomaly simulation. From Table 2, it can be inferred that the strongest change occurs for the *hot desert* (number 15) which decreases by approximately 3.4×10^6 km^2 on average over all iterations. *Savanna* (3) increases by approximately 3.3×10^6 km^2 and the *sand desert* (18) decreases by approximately 2.9×10^6 km^2. By comparing Figs. 2 and 3, it is obvious that these changes are related to a shift of vegetation at the southern edge of the Sahara, particularly in the southwest part of the Sahara, and Arabian and Indo-Pakistani deserts (the latter concerns only one or two grid boxes). The difference in *cool grass* (13) of some 2×10^6 km^2 basically concerns Central Asia. By applying the Student's t-test to the four iterations of the control run and the last four iterations

Table 2. Land area (in $10^6 km^2$) covered by each biome (for biome numbers see Table 1)

	1	2	3	4	5	6	7	8	9
01	5.42	3.89	6.22	5.85	1.56	5.05	3.88	3.89	5.05
02	4.64	6.16	4.22	4.22	3.89	4.63	4.63	5.80	5.01
03	22.34	23.43	23.05	23.44	30.73	27.25	26.15	27.28	24.63
04	6.16	4.57	3.46	4.86	4.09	5.25	4.11	5.90	4.96
05	4.69	5.44	3.94	4.77	4.47	5.32	5.02	6.07	4.80
06	5.09	5.09	5.54	5.02	5.37	6.67	4.79	5.42	6.75
07	2.81	1.54	3.06	2.01	2.56	2.73	3.06	2.18	3.25
08	11.61	10.03	11.24	10.16	12.62	13.30	10.80	10.99	11.17
09	0.99	1.24	0.50	0.75	0.99	0.25	1.24	1.24	1.27
10	0.50	0.74	1.10	1.08	1.32	0.80	0.77	0.81	2.10
11	12.64	12.53	14.03	12.80	19.30	14.79	14.82	15.20	15.98
12	7.67	6.46	6.95	7.33	7.63	6.73	9.25	6.13	8.51
13	5.98	7.44	5.93	5.56	5.60	4.18	4.81	4.20	3.35
14	15.13	17.34	17.16	17.34	15.91	16.69	17.12	17.76	15.33
15	16.22	16.58	16.58	17.19	10.89	13.20	14.19	13.06	12.47
16	1.87	1.87	1.83	1.83	0.93	0.63	1.53	1.18	1.18
17	7.29	6.69	6.24	6.84	7.64	6.57	7.14	7.29	8.22
18	9.07	9.07	9.07	9.07	4.62	6.10	6.84	5.73	6.10

Antarctica is not included in *polar desert*. Columns 1 to 4: results of the atmosphere-biome model when initialized with the present-day distribution of vegetation. Columns 5 to 9: results of the atmosphere-biome model when initialized with the anomalous vegetation distribution (see Sect. 3.1)

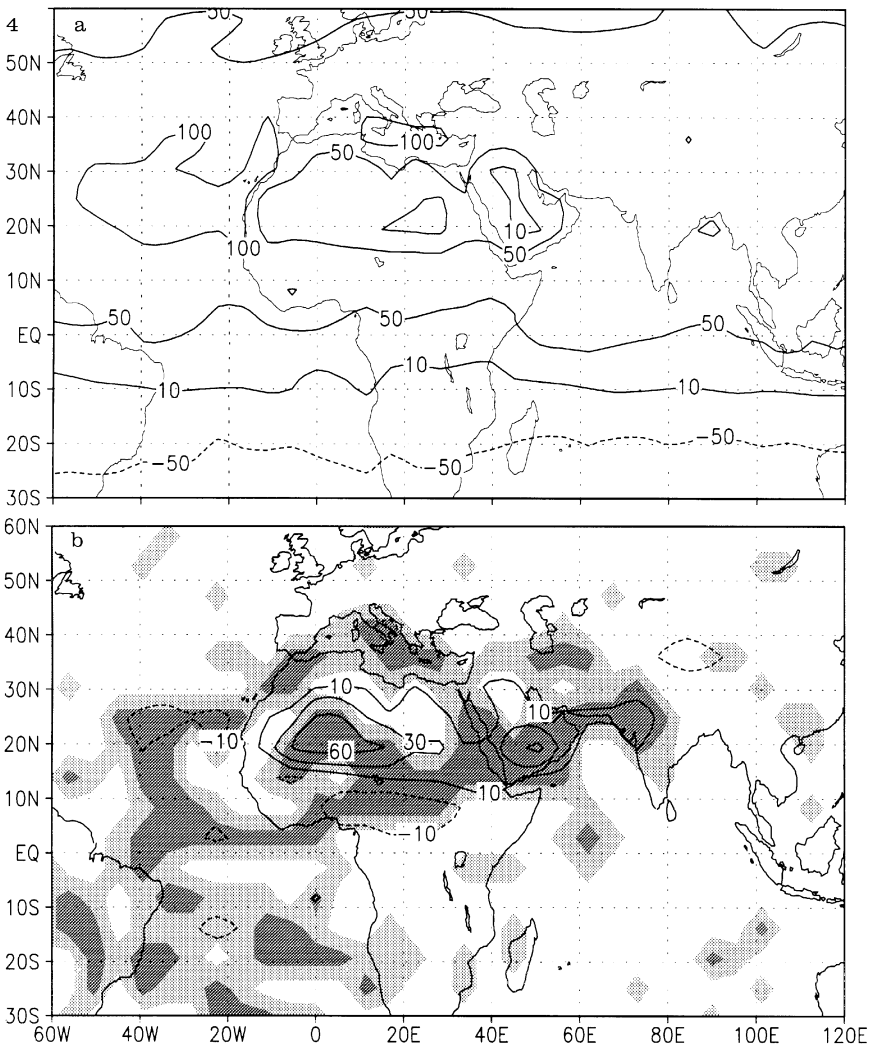

Fig. 4. a Net radiation (in W/m^2) at the top of the atmosphere during the summer month (June, July, August) on average over the four iterations of the control simulation in which the atmosphere-biome model is initialized with present-day vegetation distribution. **b** Difference in summer (June, July, August) net radiation (in W/m^2) at the top of the atmosphere between control and anomaly simulation. Results are averaged over all four iterations of the control simulation and over the last four iterations of the anomaly simulation. *Dark* (*light*) *shaded* areas indicate significant differences, estimated by a local student t-test, at a 1% (5%) significance level

of the anomaly run, it can be shown that the differences between *sand desert*, *hot desert*, *savanna*, *xerophytic woods/shrub*, and *cool grass* are significant at the 1% level. Changes in the areal extent of other biomes are not significant.

3.2 Atmospheric state

It is not unexpected that the strongest change between present-day and anomalous biome distribution occurs in the Sahel, the border between desert and savanna. Charney (1975) suggested a self-induction effect of deserts through albedo enhancement which exists when a desert has formed (see also Charney et al. 1975, 1976, 1977). As mentioned in the Introduction, a desert is a radiative sink of heat relative to its surroundings. This is clearly seen in Fig. 4a which depicts the calculated net radiation at the top of the atmosphere on average over all control simulations during the summer season (June, July, August). For the other seasons, only slight changes can be observed (not presented here). Figure 4b shows the difference between the control and the anomaly simulations indicating an increase of positive net radiation in the Sahara and southern parts of Arabia. Dark shaded areas and light shaded areas indicate where these differences are significant at the 1% and 5% level, respectively (the local Student's t-test includes the four iterations of the control run and the last four iterations of the anomaly run). A valid similarity is seen if the difference between net-radiation at the top of the atmosphere and the energy residuum at the Earth's surface is considered (not shown here).

In order to maintain thermal equilibrium, the air above a desert must descend and compress adiabatically. In Fig. 5a, the velocity potential at 200 hPa on average over the summer seasons of all control simulations is plotted. It is seen that there is a pole of divergence over Indonesia, and a pole of convergence over South Africa. This dipole pattern of the velocity potential recaptures the Hadley-Walker circulation. The difference picture (Fig. 5b) reveals a shift of this pattern associated with a decrease of convergence above East Africa and the Arabian Sea and an increase of convergence over the tropical Atlantic. The velocity potential taken at 850 hPa shows the complementary picture (not shown here) with

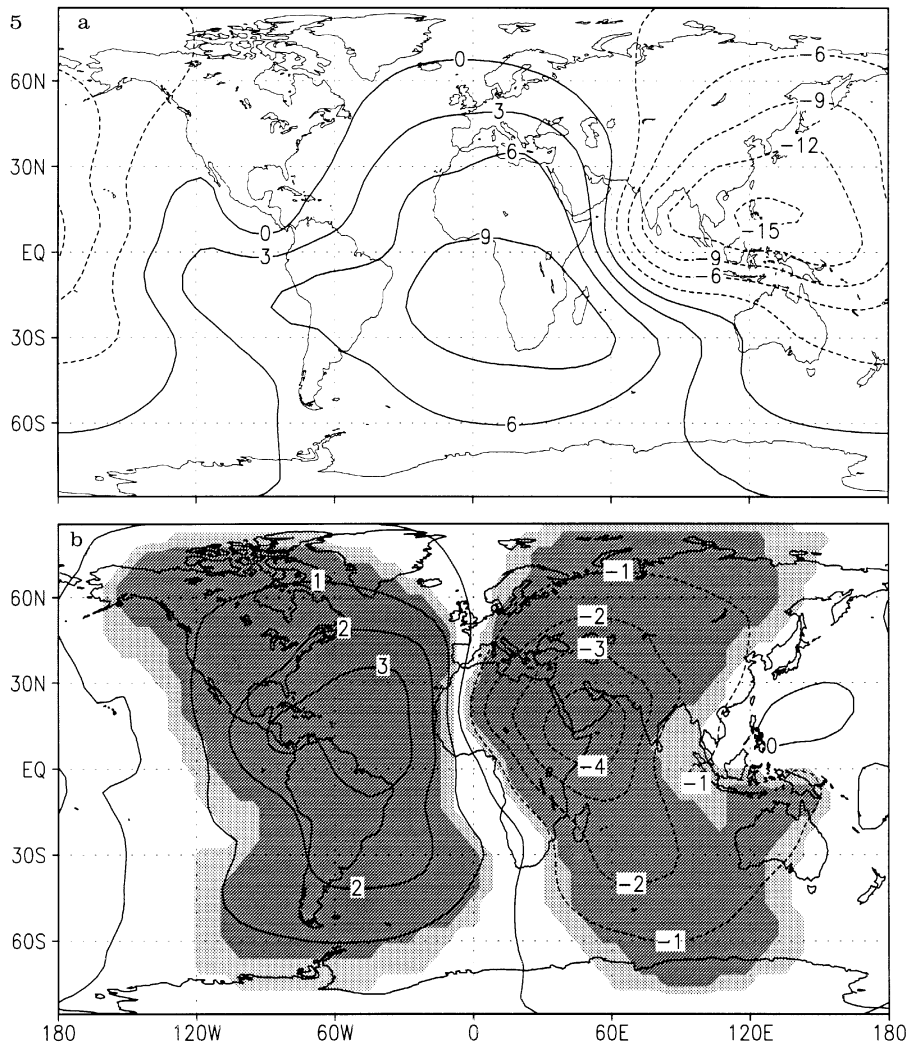

Fig. 5. a Same as Fig. 4a, except for the velocity potential (in km^2/s) at 200 hPa. **b** Same as Fig. 4b, except for differences in velocity potential

an increase of convergence over East Africa and a decrease over the tropical Atlantic. Hence this pattern corroborates a shift of descending and ascending (or less descending) motion associated with a shift of vegetation into deserts.

As a consequence of the shift in the Hadley-Walker circulation, the African and Indian summer monsoon increases in its strength (not plotted here), and the precipitation patterns between control and anomaly simulation differ. Monthly means of precipitation (in units mm/ month) on average over June, July, August are given in Fig. 6a. The ITCZ (Intertropical Convergence Zone) over Africa as well as the intense rainfall pattern over Indonesia are fairly well reproduced by ECHAM. Only the amount of rain over Africa and over India is underestimated (for details see Roeckner et al. 1992) With a north/northeastward shift of vegetation and enhanced African summer monsoon, the rainfall over the SW Sahara increases by some 100 mm/month and it decreases over the tropical North-Atlantic (see Fig. 6b). There is also a strong and significant increase of precipitation over the Indian subcontinent although there is little change in vegetation between control and anomaly simulations. Following Meehl (1994), it is argued (see later) that there is a positive feedback between increased soil moisture and Indian summer monsoon. Figure 7a, b depicts the relative soil moisture and how it differs between control and anomaly climate. The increase in soil moisture is largest over both the SW Sahara and the Indian subcontinent.

3.3 Surface energy budget

Ripley (1976) criticizes Charney's hypothesis of a negative feedback between albedo and precipitation. He argues that Charney et al. (1975) have ignored the effect of vegetation on evapotranspiration. In fact, Charney et al.'s (1975, 1977) model does not represent vegetation in any manner except as changing albedo. Moreover, soil moisture is not interactively modeled, but simply prescribed. Ripley points out that vegetated surfaces are usually cooler than bare ground, because the darker vegetated surface would absorb more solar radiation which is mainly used for

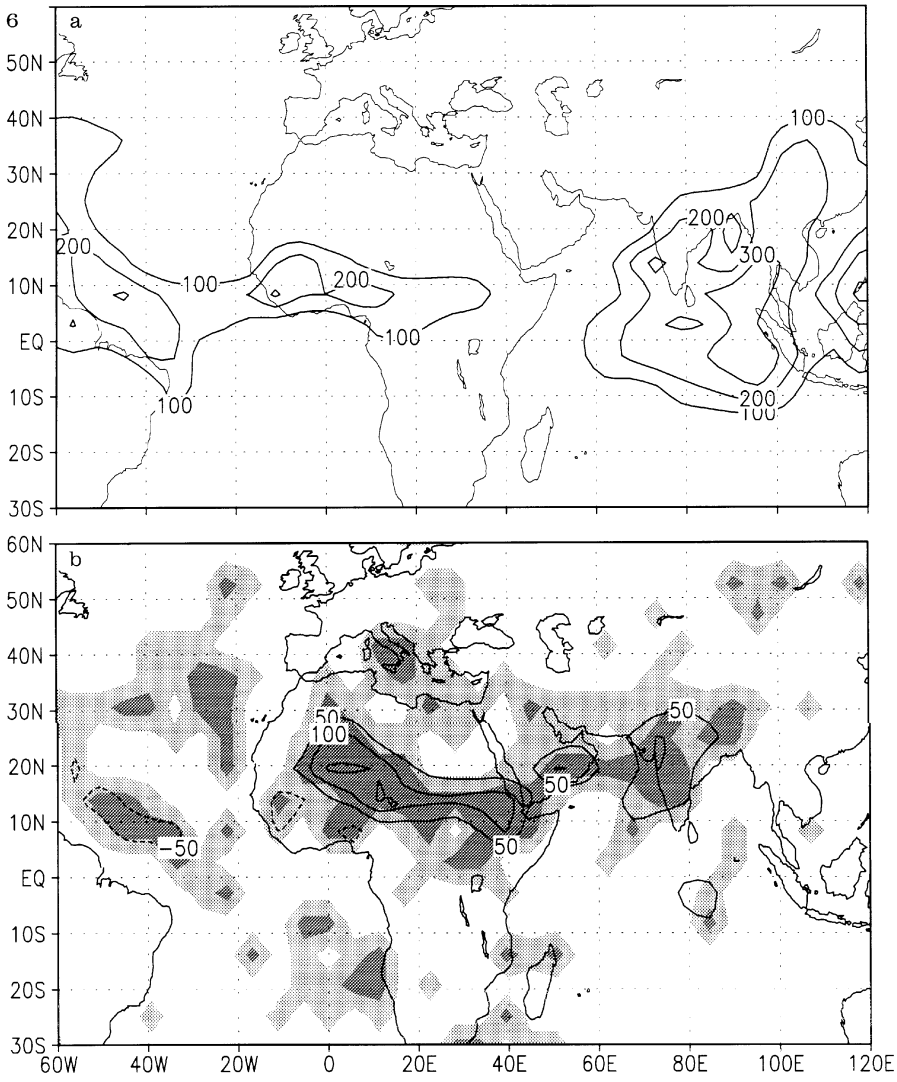

Fig. 6. a Same as Fig. 4a, except for precipitation (in mm/month). **b** Same as Fig. 4b, except for differences in precipitation

evaporatranspiration. The cooler surface, in turn, would reduce rather than increase convection and precipitation. In their reply, Charney et al. (1976) emphasize that it is not merely the surface temperature, but the total flux of sensible and latent heat to the atmosphere and, subsequently, changes in moist static energy ($c_pT + Lq + gz$, where c_p is the specific heat capacity of the atmosphere at constant pressure, T is the absolute temperature, L is the specific latent heat of evaporation, q is the specific humidity, g is the acceleration of gravity, and z is the height above ground) in the lower atmospheric layers which determine convective rainfall. Charney et al. (1975, 1977) argue that mainly the latent heat flux and, hence, the moist static energy increase with decreasing albedo. They demonstrate this effect by sensitivity studies, i.e., by prescribing wet soil in the case of a vegetated surface. Since there is an interactive soil-vegetation model in ECHAM, these arguments can be tested in detail.

In Table 3, the surface energy budget for the summer months on average over the SW-Sahara and on average over the Indian subcontinent are listed. These regions are chosen, because both regions experience a large increase in precipitation and soil moisture in the anomaly simulation versus the control simulation (see Figs. 6, 7). However, a strong change in the radiative fluxes at the top of the atmosphere is found only over the SW Sahara. Over the Indian subcontinent, only the western part which comprises the Pakistani desert is affected by a change in the atmospheric radiation budget (see Fig. 4). For the control run, values of the surface energy budget are averaged over all four iterations, and for the anomaly run, over the last four iterations. All differences between values of the control and of the anomaly run are significant at a 1% level, except for the difference between surface temperatures in the SW Sahara which is significant at the 5% level and the exception for the sensible heat fluxes in the same region which is not significant.

In the SW Sahara, there is a strong difference in surface parameters between anomaly and control simulation; these differences are much smaller over the Indian subcontinent, particularly, concerning albedo. As a consequence, in the SW Sahara, the net radiation is larger in the anomaly simulation than in the control simulation. The

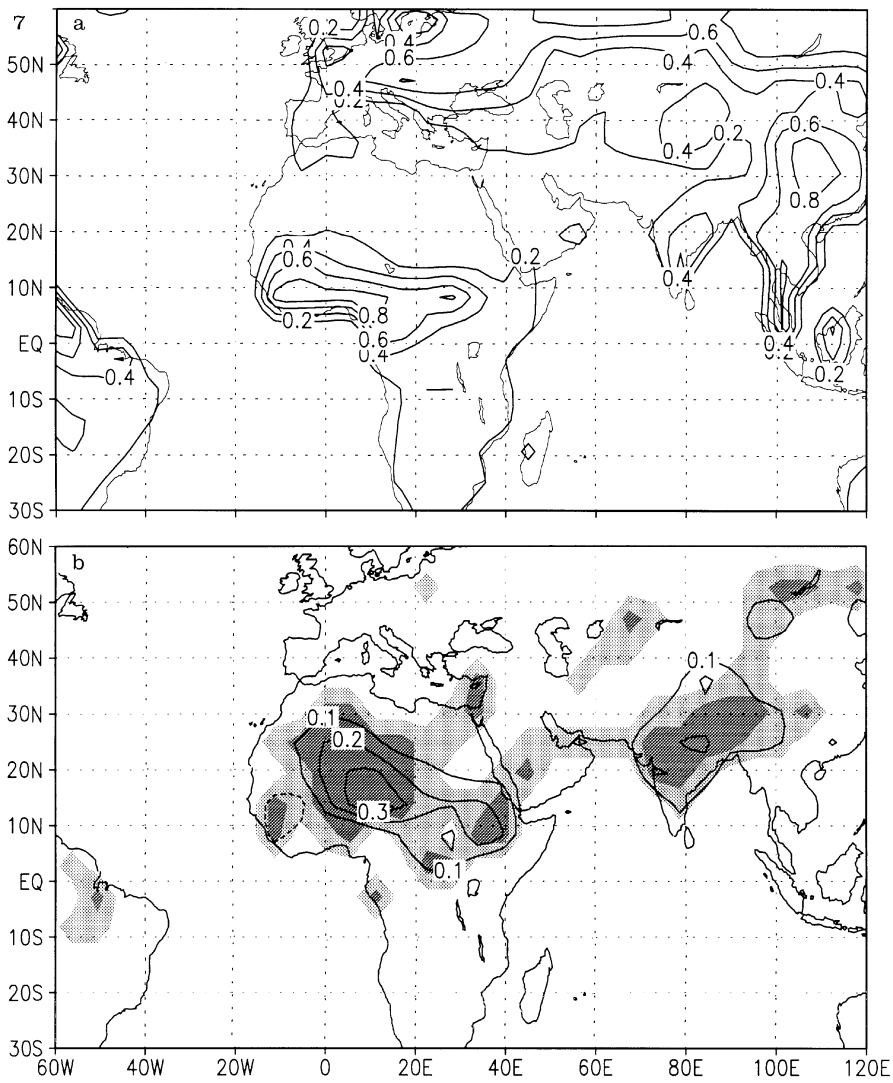

Fig. 7. a Same as Fig. 4a, except for relative soil moisture. **b** Same as Fig. 4b, except for differences in relative soil moisture

Table 3. Surface parameters and surface energy and water fluxes on average over the SW-Sahara (approximately 17 °N – 28 °N, 10 °W – 20 °E) and over the Indian subcontinent (10 °N – 28 °N, 70 °E – 87 °E)

	SW Sahara		India	
	Control	Anomaly	Control	Anomaly
Albedo	0.35	0.24	0.17	0.16
Roughness length	0.004	0.040	0.144	0.222
LAI	0.0	1.4	2.3	2.7
Vegetation ratio	0.00	0.35	0.59	0.66
Incident shortwave radiation	336	299	273	256
Outgoing shortwave radiation	− 118	− 64	− 47	− 42
Net shortwave radiation	218	235	226	214
Atmospheric radiation	368	396	414	418
Outgoing thermal radiation	− 504	− 496	− 491	− 482
Net thermal radiation	− 136	− 100	− 77	− 64
Net radiation	82	136	149	150
Sensible heat flux	− 48	− 47	− 40	− 20
Latent heat flux	− 6	− 70	− 92	− 124
Evapotranspiration	7	72	95	129
Precipitation	10	98	168	240
Relative soil moisture	0.12	0.31	0.39	0.57
Surface temperature	35.4	33.7	32.0	29.8
Moist static energy	3.18	3.29	3.40	3.46
Cloud cover	0.19	0.43	0.54	0.63

Values are averages over the summer months (June, July, August) and averages over the four iterations of the control simulation and over the last four iterations of the anomaly simulation, respectively. Roughness lengths have the dimension (m), energy fluxes are given in (W/m^2) (negative values indicate upward fluxes), water fluxes are given in (mm/month), temperatures in (°C), and moist static energy (at 2 m above ground) in 10^5 (J/kg).

vegetated surface (of the anomaly simulation) receives less solar radiation due to higher cloudiness than in the control simulation, but it reflects less solar radiation. The slight increase in energy flux to the earth surface due to net solar radiation is increased by a stronger atmospheric radiation caused by higher cloudiness, and less outgoing thermal radiation. This energy surplus is used to increase evaporation. The sensible heat flux shows no significant change.

There is little change in net radiation over the Indian subcontinent. In the control simulation, the already vegetated surface receives more solar radiation due to less cloud cover than in the anomaly simulation, but it loses more energy due to larger thermal radiation from the surface. Only the Bowen ratio decreases in this region, presumably due to the increase in soil moisture which is available for evapotranspiration. In both regions, evapotranspiration leads to lower surface temperatures and to an increase in moist static energy which in turn amplifies convective rainfall. Precipitation exceeds evapotranspiration and this effect is larger in the anomaly simulation than in the control simulation. Hence, atmospheric moisture must be advected by the African and Indian summer monsoon which becomes stronger in the anomaly simulation. This corroborates Meehl's (1994) assertion of a positive feedback between increased soil moisture and a stronger Indian summer monsoon. In contrast to Meehl's (1994) model results, however, the temperature contrast between land and ocean is decreased. Meehl (1994) mentions that this difference could have to do with the difference between the types of convection scheme used in different models.

4 Conclusion

The results of this study suggest that under present-day conditions of solar irradiation and sea-surface temperatures, at least two solutions of the ECHAM-BIOME model are possible: the present-day solution and an anomalous solution. The former is associated with the present-day distribution of vegetation and deserts and the latter, with savanna and xerophytic shrub in the southern part of the Sahara and Arabian and Indian deserts, all else being similar. The difference between biome patterns are caused by a change in the radiation budget of the air above the 'green desert' and by a subsequent change in large-scale vertical motion and surface moisture fluxes, for the sub-Saharan region. This is in keeping with the mechanism of a positive bio-geophysical feedback proposed by Charney (1975). Dickinson (1992) questions whether Charney's (1975) hypothesis would apply to all semi-arid regions as it includes only the role of atmospheric moisture convergence, but not surface moisture fluxes. In other regions, changes in moisture convergence could enhance or cancel the effects of increased evapotranspiration in modifying rainfall which could be quite dependent on details of the regional climate. Since changes in other semi-arid regions appear to be marginal in this study, Dickinson's (1992) conjecture could not be explored in detail. For the Indian subcontinent, however, a positive feedback between increased soil moisture and stronger summer monsoon is found in the ECHAM-BIOME model. Such a positive internal feedback has been mentioned by Meehl (1994).

The question remains whether the existence of two solutions is realistic. Since validation is not possible, it remains to be critically assessed whether the assumptions on which the ECHAM-BIOME model is based are realistic.

One *caveat* is that the biome model is a static model. The ECHAM-BIOME model cannot deal with transient vegetation dynamics, it merely predicts equilibrium states. Hence, the ECHAM-BIOME model does not tell how the vegetation intrudes into deserts. If such an intrusion is unlikely to happen under present-day conditions, then it seems hardly possible that the anomalous state will occur in reality. Careful analysis of vegetation in North Africa reveals that the boundaries of the Sahara appear rather stable in the last 130 years (Schulz and Hagedorn 1994). On the other hand, there is evidence from paleo-climatological records that the vegetation in the Sahara has changed during the Holocene (e.g., Crowley and North, 1991) which may be related to changes in orbital parameters (Kutzbach and Guetter 1986).

Secondly, the ECHAM-BIOME model allows for changes in vegetation structure only, changes in soil properties are not taken into account. This limitation is serious if changes in the tropical rain forest are considered. In the rain forest, the largest portion of the biomass is found in the plants and only little in the soil. Deforestation of rain forest necessarily implies degradation of soil. Therefore, the stability of the rain forest in this ECHAM-BIOME model, *tropical rain forest* and *tropical seasonal forest* is predicted to occur under present-day as well as under anomalous conditions, is questionable. Artificial aforestation of deserted regions, on the other hand, seems feasable. Within this context, the problem of defining the new biome *sand desert* must also be readdressed. So far, definition of *sand desert* in terms of climate and soil types has not been successful.

Thirdly, there is no ocean response in the ECHAM-BIOME model. Since Lamb and Peppler (1992) found a correlation between sub-Saharan rainfall and SST of the tropical Atlantic, one cannot exclude that there is a feedback between ocean dynamics and large-scale vegetation changes. On the other hand, the results obtained from a coupled atmosphere-ocean GCM by Hoffmann et al. submitted (1995) show just marginal effects of tropical deforestation on the large-scale air–sea interaction. The latter result is certainly suggestive, but not conclusive, hence more experimentation must be done.

The main conclusion of this study is that an equilibrium-response atmosphere-biome model reveals multiple solutions in the African and Indian monsoon region depending on the initial land-surface conditions. The *caveats* mentioned do not reveal serious draw backs of the present study, rather they indicate the direction further research must follow.

Acknowledgements. The author would like to thank Colin Prentice, Department of Plant Ecology, Lund University, Sweden, for making the BIOME model available. Thanks are also due to Claudia Kubatzki, Universität Hamburg, and Uwe Schulzweida, Max-Planck-Institut für Meteorologie, for programming assistance. The author very much appreciates constructive comments by Lydia Dümenil, Max-Planck-Institut für Meteorologie, and by two anonymous reviewers.

References

Charney JG (1975) Dynamics of deserts and drought in the Sahel. Q J R Meteorol Soc 101 : 193–202

Charney JG, Stone PH, Quirk WJ (1975) Drought in the Sahara: a biogeophysical feedback mechanism. Science 187 : 434–435

Charney JG, Stone PH, Quirk WJ (1976) Reply. Science 191 : 100–102

Charney JG, Quirk WJ, Chow S-H, Kornfield J (1977) A comparative study of the effects of albedo change on drought in semi-arid regions. J Atmos Sci 34 : 1366–1385

Claussen M (1994) Coupling global biome models with climate models. Clim Res 4 : 203–221

Claussen M (1996) Variability of global biome patterns as function of initial and boundary conditions in a climate model. Clim Dyn 12 : 371–379

Claussen M, Esch M (1994) Biomes computed from simulated climatologies. Clim Dyn 9 : 235–243

Cramer W (1995) Using plant functional types in a global vegetation model. In: Smith TM, Shugart HH, Woodward FI (eds) (forthcoming) Plant functional types. Cambridge University Press, Cambridge, England

Crowley TJ, North RN (1991) Paleoclimatology. Oxford Monographs on Geology and Geophysics 18, Oxford University Press, New York

Dickinson RE (1992) Changes in land use. In: Trenberth KE (ed) Climate system modeling. Cambridge University Press, Cambrige, pp 698–700

Gates WL (1992) AMIP: the atmospheric model intercomparison project. Bull Am Meteorol Soc 73 : 1962–1970

Henderson-Sellers A (1993) Continental vegetation as a dynamic component of global climate model: a preliminary assessment. Clim Change 23 : 337–378

Hoffmann G, Claussen M, Latif M, Stockdale T (1995) Does tropical deforestation affect large-scale air–sea interactions? J Clim submitted

Kutzbach J, Guetter (1986) The influence of changing orbital parameters and surface boundary conditions on climate simulations for the past 18 000 years. J Atmos Sci 43 : 1726–1759

Lamb PJ, Peppler RA (1992) Further case studies of tropical Atlantic surface atmospheric and oceanic patterns associated with sub-Saharan drought. J Clim 5 : 476–487

Leemans R, Cramer W (1991) The IIASA database for mean monthly values of temperature, precipitation, and cloudiness on a global terrestrial grid. IIASA Research Report RR-91-18, Laxenburg, Austria

Meehl GA (1994) Influence of the land surface in the Asian summer monsoon: external conditions versus internal feedbacks. J Clim 7 : 1033–1049

Monserud RA, Leemans R (1992) Comparing global vegetation maps with Kappa statistic. Ecol Modell 62 : 275–293

Monteith JR (1973) Principals of enviromental physics, Elsevier, New York

Olson JS, Watts JA, Allison L J (1983) Carbon in live vegetation of major world ecosystems. ORNL-5862, Oak Ridge National Laboratory, Oak Ridge

Prentice IC, Cramer W, Harrison SP, Leemans R, Monserud RA, Solomon AM (1992) A global biome model based on plant physiology and dominance, soil properties and climate. J Biogeog 19 : 117–134

Ramanathan V, Cess RD, Harrison EF, Minis P, Barkstrom BR, Ahmad E, Hartmann D (1989) Cloud-radiative forcing and climate : results from the Earth Radiation Budget Experiment. Science 243 : 57–63

Roeckner E, Arpe K, Bengtsson L, Brinkop S, Dümenil L, Kirk E, Lunkeit F, Esch M, Ponater M, Rockel B, Sausen R, Schlese U, Schubert S, Windelband M (1992) Simulation of the present-day

climate with the ECHAM model: impact of model physics and resolution. Report 93, Max-Planck-Institut für Meteorologie, Hamburg

Ripley EA (1976) Drought in the Sahara: insufficient biogeophysical feedback. Science 191 : 100

Schulz E, Hagedorn H (1994) Die Wüste –wächst sie denn wirklich? Geowissenschaften 12 : 204–212

Shukla J (192) GCM response to changes in the boundary conditions at the Earth's surface: a review. In: Second International Conference on Modelling of Global Climate Change and Variability, Abstracts. Max-Planck-Institut für Meteorologie, Hamburg